Spinning Disc Confocal Microscopy in the NIR-II Window

Overview

Near-infrared (NIR) fluorescence is a technique used widely within biological and medical research due to the fact that NIR light can penetrate deeply in biological specimens. It offers high spatiotemporal resolution alongside the capability to image quickly (Fan 2019). The second NIR window (NIR-II, 900 – 1700 nm) is of recent interest due to its superior penetration depth, reduced tissue absorption and decreased photon scattering compared to the visible and shorter NIR wavelength range (Fan 2019, Carr 2018, Diao 2015, Hong 2014). This is because photon scattering is scaled within biological tissues via $\lambda^{-\alpha}$ (where α = 0.2–4 dependent on tissue type) (Fan 2019, Diao 2015). NIR-II wavelengths also reduce background autofluorescence, with background autofluorescence becoming negligible with wavelengths above 1500 nm. However, the absorbance of water increases above 1400 nm, therefore, the optimal region for NIR imaging in biological tissues is between 800 and 1400 nm, resulting in better spatial resolution and penetration depths (Fan 2019, Zhu 2019).

Specialized fluorescent probes emitting within the NIR-II range have been developed by researchers in the last few years. Those used encompass quantum dots (Bruns 2017), organic dyes (Carr 2018), and single-walled carbon nanotubes (SWCNT) (Takeuchi 2019). Imaging of these fluorophores requires cameras sensitive to NIR-II wavelengths. Due to the size of the bandgap, silicon-based camera sensors are not sensitive to light above 1100 nm. Scientific cameras based on InGaAs FPAs have a high quantum efficiency in the 900 – 1700 nm wavelength range, therefore, they are optimal for NIR fluorescence imaging (Smith 2009).

Over the past decade, new NIR-II probes are being developed, with more techniques being explored from *in vivo* imaging to optical microscopy. A research group at École Polytechnique Fédérale de Lausanne (EPFL), led by Prof. Ardemis A. Boghossian, has published an article showcasing the first spinning-disc confocal light microscopy (SDCLM) in the NIR-II optical window (Zubkovs 2018). The first author of this work, Dr. Vitalijs Zubkovs, has compared optical resolution of the SDCLM with a wide-field NIR-II microscope, allowing for fast, real-time image acquisition. Through the use of a cooled InGaAs FPA camera coupled to a NIR-II optimized spinning-disc module (SDCLM-InGaAs), they demonstrated the benefits of the device in three applications:

1. single-particle tracking of NIR fluorescent nanoparticles
2. spatial distribution determination of internalized NIR fluorescent nanoparticles within an organelle
3. optical detection of glucose using single-walled carbon nanotubes (SWCNT)-based optical sensors.

SDCLM

SDCLM is a confocal microscope with additional spinning disc with multiple pinholes etched onto the surface, as shown by the schematic in Figure 1. When spun at high speeds, these pinholes allow for images to be acquired across a much larger surface area. This increases the speed of acquisition and reduces any photo damage of the sample. By varying pinhole size, disc speed and pinhole spacing alterations in image contrast, brightness and quality can be controlled. To learn more about the different types of SDCLM please see the Educational Resource by Teledyne Photometrics (https://www.photometrics.com/learn/spinning-disk-confocal-microscopy).

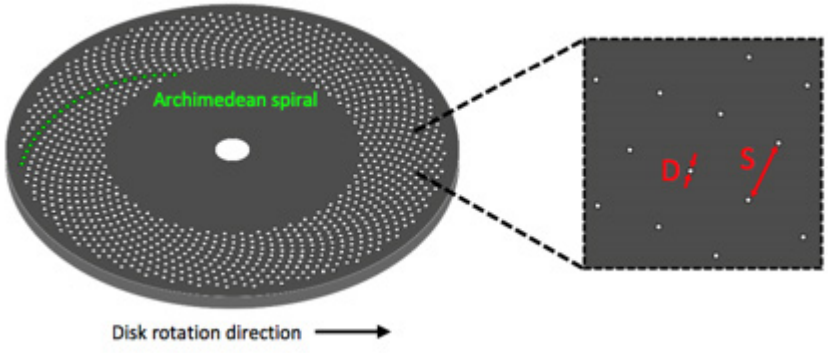

Figure 1: *A schematic of a standard Nipkow-Petran disc used for SDCLM imaging. Multiple pinholes are etched onto the disc surface to allow for fast image acquisition of large surface areas. Pinholes have a diameter D and a spacing S. Adapted from Teledyne Photometrics application note What Is Spinning Disk Confocal Microscopy?*

The EPFL team measured lateral and axial resolutions of the setups and compared it to the theoretical values which were calculated in Equations 1 and 2.

$$r_x = F_x \frac{\lambda_{EM}}{NA} \qquad 1$$

$$r_z = F_z \frac{\lambda_{EM}}{n - \sqrt{n^2 - NA^2}} \qquad 2$$

where r_x and r_z are the resolution in the lateral (x-axis) and axial (z-axis) direction respectively, F_x and F_z are the FWHM pre-factor in the lateral and axial direction (determined by the diameter of the pinholes on the spinning-discs), λ_{EM} is the wavelength, and NA is the numerical aperture.

SDCLM Experimental Setup with NIR-II

The EPFL researchers coupled an InGaAs camera (NIRvana-ST, Teledyne Princeton Instruments) to a spinning-disc module (CrestOptics) fixed on a microscope body (Nikon Eclipse), shown in Figure 2. Traditional light microscopes typically do not have anti-reflective optics in the NIR-II region; therefore, the throughput of photons is minimized due to absorption from the optical components. Hence, coating of the lens within the spinning-disc confocal was imperative to maximize photon throughput.

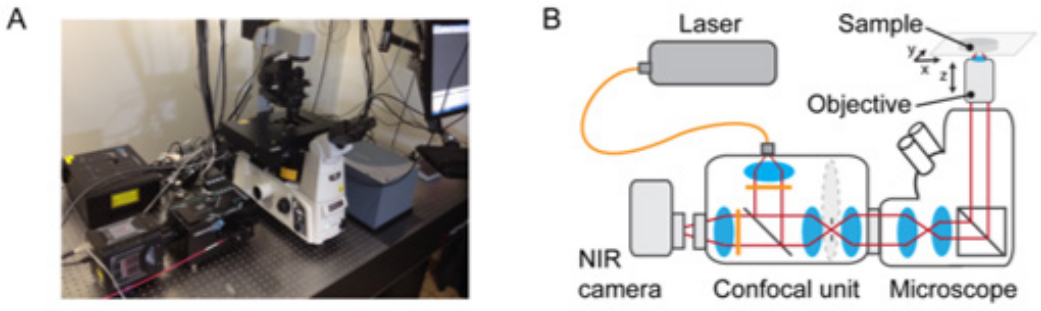

Figure 2: (A) Image and (B) optical layout of the SDCLM-InGaAs system used by the team of researchers at EPFL. Adapted from Zubkovs *et al.* (Zubkovs 2018).

SDCLM systems are advantageous as they enable fast image acquisition with higher lateral and axial resolution than wide-field imaging. The spinning-disc within the system is designed to achieve a maximum theoretical acquisition speed of approximately 18000 fps (~50 µs exposure time). This requires the disc to rotate at a speed of 15000 RPM. By using an InGaAs camera with a frame rate of 110 fps (9 ms), the researchers were able to establish an optimal acquisition time of 20 fps (50 ms) to image NIR beads with acceptable signal-to-noise ratio.

Data and Results

Using this system, the researchers at EPFL used a wide-field microscope with an InGaAs camera to image two neighboring NIR fluorescent beads immersed within oil. When the distance between the beads was less than 600 µm, they were not optically resolved in the wide-field system. However, the SDCLM-InGaAs system provided an improvement in contrast of the obtained image, improving the separation between the beads, as shown in Figure 3. Measured lateral and axial resolutions in the SDCLM microscope at 980 nm were 0.5±0.1 µm and 0.6±0.1 µm respectively. There was a 17% improvement in the lateral resolution and 45% in the axial resolution in comparison to the wide-field system.

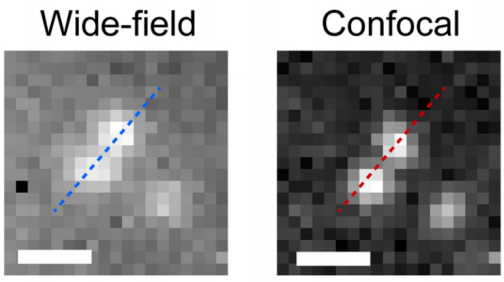

Figure 3:*Wide-field and SDCLM-InGaAs confocal images of 186 ± 48 nm NIR fluorescent beads showing improved image contrast with the SDCLM-InGaAs system. Intervals of the pixel intensities of the images were adjusted to the same values. Scale bar is 1 µm. Adapted from Zubkovs et al. (Zubkovs 2018).*

Improvement in axial resolution, caused by the SDCLM-InGaAs system, allowed for more accurate determination of the diffusion coefficients of the NIR fluorescent beads. Diffusion coefficients measured in the SDCLM were closer to the theoretical value in comparison to wide-field tracking. For example, the median diffusivity of the beads in water was determined by following their trajectories on time-laps images. The value obtained from the SDCLM images was ~25% higher than that based on wide-field images.

Enhancement in spatiotemporal resolution in the NIR region could expand new horizons in studies which involve *in vitro* and *in vivo* imaging. In the recent decades, many biological and medical studies focus on understanding living cell and nanoparticle interaction better. Some cells are able to uptake functionalized particles that penetrate organelles inside the cell (Feng 2019, Kodiha 2015, Chen 2019). Organelles which are present in plant cells are chloroplasts, which are an interesting subject to study because of their light energy harvesting bio-function. As chloroplasts absorb over a wide range of visible light, and also autofluoresce, it becomes challenging to image any chloroplast-internalized particles labeled with visible dyes. Therefore, NIR-II fluorophores, such as SWCNTs, can be employed in nanoparticle uptake studies to draw more accurate conclusions on how nanoparticle surface functionalization promotes or inhibits their uptake in organelles. The SDCLM-InGaAs microscope allowed for clearer localization of SWCNTs within chloroplasts through improved resolution and contrast – indicating that a DNA coating was optimal for SWCNT uptake.

The EPFL team pioneered the demonstration of the first spatiotemporal glucose nanosensor, which allowed the tracking of axial diffusion of glucose in agarose gel at the microscopic level. In the future, such sensors could be immobilized within a gel matrix and implanted *in vivo* for continuous analyte monitoring (Marchetti 2020, Zhang 2019, Kamanina 2019). For example, glucose oxidase (GOx) enzyme-functionalized SWCNTs can be used as glucose-specific sensors (Zubkovs 2017, Kamanina 2019). Changes in the fluorescence intensity of the GOx-SWCNT nanosensors is proportional to the change in glucose concentration. During the experiment, as the glucose diffused and interacted with the GOx-SWCNTs dispersed within the gel matrix, the SDCLM-InGaAs microscope monitored the sensor response at different axial sections of the gel, as shown in Figure 4. Although this can also be achieved via wide-field imaging, SDCLM imaging allowed for smaller axial segments to be imaged giving a more representative diffusion gradient.

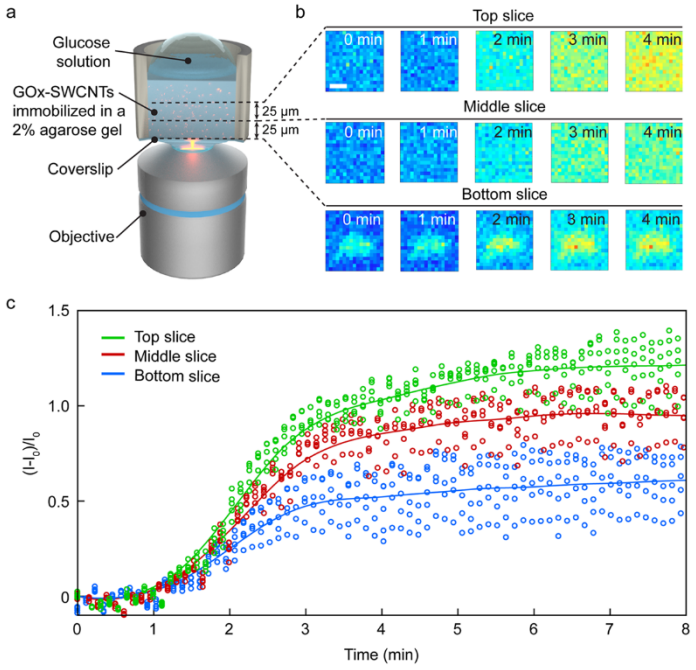

Figure 4:The spatiotemporal response of GOx-SWCNT biosensors to glucose. (A) Schematic of the system, with GOx-SWCNTs immobilized in an agarose gel. (B) Confocal images of NIR fluorescent GOx-SWCNT clusters with fluorescent increase triggered by glucose concentration. (C) Normalized fluorescence intensity of five GOx-SWCNT clusters at each of the three axial positions after the addition of glucose. Adapted from Zubkovs *et al*. (Zubkovs 2018).

Conclusion

The researchers at EPFL have clearly demonstrated that the use of a SDCLM in combination with an InGaAs camera will be highly beneficial to biological and medical research, especially when investigating *in vitro* and *in vivo* biosensors. NIR-II is the perfect wavelength range to obtain high-resolution images of biological tissue with reduced photon scattering, autofluorescence and increased penetration depth. Merging optical microscope techniques, such as SDCLM to increase image acquisition times and scanning surface area, and sensitive cameras, such as InGaAs, high resolution real-time imaging of biological tissues and bioprocesses can be achieved.

As InGaAs cameras are highly sensitive within the 900 – 1700 nm range they are ideal for NIR-II imaging. InGaAs cameras are also advantageous as they are deep-cooled to reduce dark noise. Dark noise is the noise produced from the electric current flowing through photosensitive devices. Further information regarding InGaAs FPA cameras and their advantages can be found in the Technical Note by Teledyne Princeton Instruments (https://www.princetoninstruments.com/userfiles/files/technotes/Introduction-to-scientific-InGaAs-FPA-cameras.pdf)

References

Bruns O, et al., Next-generation in vivo optical imaging with short-wave infrared quantum dots, *Nature Biomedical Engineering*, 4, **2017**

Carr J.A., et al., Shortwave infrared fluorescence imaging with the clinically approved near-infrared dye indocyanine green, *Proceedings of the National Academy of Sciences of the United States of America*, 115, **2018**

Chen H, et al., Functionalized Spiky Particles for Intracellular Biomolecular Delivery, *ACS Central Science*, 5, **2019**

Diao S, et al., Fluorescence Imaging In Vivo at Wavelengths beyond 1500 nm, *Angewandte Chemie*, 54, **2015**

Fan Y, Zhang F., A New Generation of NIR-II Probes: Lanthanide-Based Nanocrystals for Bioimaging and Biosensing, *Advanced Optical Materials*, 7, **2019**

Feng Q, Lee S, Kornmann B., A toolbox for organelle mechanobiology research – Current needs and challenges, *Micromachines*, 10, **2019**

Hong G, et al., Through-skull fluorescence imaging of the brain in a new near-infrared window, *Nature Photonics*, 8, **2014**

Kodiha M, et al., Off to the organelles – killing cancer cells with targeted gold nanoparticles, *Theranostics*, 5, **2015**

Marchetti M, et al., Immobilization of Allantoinase for the Development of an Optical Biosensor of Oxidative Stress States, *Sensors,* 20, **2019**

Smith A, Mancini M, Nie S., Bioimaging: Second window for in vivo imaging, *Nature Nanotechnology*, 4, **2009**

Takeuchi T, et a., Characterization and Biodistribution Analysis of Oxygen-Doped Single-Walled Carbon Nanotubes Used as *in Vivo* Fluorescence Imaging Probes, *Bioconjugate Chemistry*, 30, **2019**

Zhang J, et al., An acetylcholinesterase biosensor with high stability and sensitivity based on silver nanowire-graphene-TiO2 for the detection of organophosphate pesticides, *RSC Advances*, 9, **2019**

Zhu B, et al., Comparison of NIR versus SWIR fluorescence image device performance using working standards calibrated with SI units, *IEEE Transactions of Medical Imaging*, **2019**

Zubkovs V, et al., Mediatorless, Reversible Optical Nanosensor Enabled through Enzymatic Pocket Doping, *Small*, 13, **2017**

Zubkovs V, et al., Spinning-disc confocal microscopy in the second near-infrared window (NIR-II), *Scientific Reports*, 8, **2018**